GSA Data Repository Item 2020192

Pohl, A., Donnadieu, Y., Godderis, Y., Lanteaume, C., Hairabian, A., Frau, C., Michel, J., Laugie, M., Reijmer, J.J.G., Scotese, C.R., and Borgomano, J., 2020, Carbonate platform production during the Cretaceous: GSA Bulletin, https://doi.org/10.1130/B35680.1.

Data Repository

Sections S1 to S2:

S1. Geological database of Cretaceous carbonate preservation rates

S2. The GEOCLIM model

Supplementary Figures S1 to S2:

Figure S1. Mean preservation rates calculated using time bins of 5 m.y.

Figure S2. Continental reconstructions used in the GEOCLIM model (Scotese, 2016; Scotese and Wright, 2018).

Supplementary Tables S1 to S2:

Table S1. Compilation of neritic carbonate preservation rates.

Table S2. Table of the 89 climatic experiments conducted with the FOAM model. Each experiment was run until deep-ocean equilibrium (≥2000 model years). The past 50 years were used to build the monthly climatology files used for the analyses. Model output is available in numerical (netcdf) format at https://doi.org/10.1594/PANGAEA.904255.

S1. Geological database of Cretaceous carbonate preservation rates

The database content is shown in Figure 1 in the main text. Mean preservation rates calculated using 5-m.y. time bins are given in Fig. S1. Raw data can be found in Table S1. This new database for carbonate preservation rates was created from the literature. To calculate the rate of preservation we divided the thickness by the stratigraphic interval duration (Bosscher and Schlager, 1993). The overall stratigraphic thicknesses were used. Compaction was not corrected for because it was not sufficiently well constrained. As a result, rates were surely underestimated. Duration estimates came from the stratigraphic boundaries described in the literature (Gradstein et al., 2012).

S2. The GEOCLIM model

The GEOCLIM model is a climate-carbon cycle model that asynchronously couples a carbon cycle box model with a general circulation model. Because the ocean-atmosphere general circulation model could not be run for several million years due to excessive computation time, we first ran climatic simulations for each time slice/paleogeography with several CO_2 levels (70 - 8960 ppm) and gathered them in a catalog of simulations (one catalog per time slice/paleogeography). We then interpolated between the different members of the lookup table all along the 10-million-year-long integration of the carbon cycle model to obtain climatic variables required for the computation of continental weathering (i.e., temperature and runoff) for any CO_2 value within the covered CO_2 range.

The carbon cycle box model is the COMBINE model upgraded following Donnadieu et al. (2006). The oceans are modeled by 9 "boxes". Four boxes represent the photic and deep ocean zones for the northern and southern high-latitude regions. Three boxes represent the low to mid-latitude open-ocean photic zone, thermocline, and deep ocean. Two boxes represent the low to mid-latitude photic zone and deep epicontinental reservoirs. A 10th box represents the atmosphere.

The climatic component of GEOCLIM is the FOAM ocean-atmosphere model version 1.5 (Jacob, 1997), a mixed-resolution general circulation model. The atmospheric component of FOAM is a parallelized version of the National Center for Atmospheric Research's (NCAR) Community Climate Model 2 (CCM2) with radiative and hydrologic physics upgrades after CCM3 version 3.2. It uses a R15 spectral resolution (4.5° × 7.5°) with 18 levels in the vertical dimension. The ocean model is the Ocean Model version 3 (OM3). It is a 24-level z-coordinate ocean general circulation model, run at a 1.4° × 2.8° resolution.

Our setup of the GEOCLIM model is very similar to the one previously used by Donnadieu et al. (2006), with the following exceptions. We used the version of the FOAM model that resolves ocean dynamics, whereas Donnadieu et al. (2006) used the slab mixed-layer model. We followed the recent study by Suchéras-Marx et al. (2019) by considering that calcifying plankton was already well-established in open-ocean settings during the Early Cretaceous (Ridgwell, 2005; Ridgwell and Zeebe, 2005). Lastly, we did not rely on Walker et al. (2002) to provide an estimate of the area of shallow-marine carbonates (see Equation 1 in main text), rather, we assumed that the area of the carbonate platforms varied proportionally with the area of the shallow-marine environments available to carbonate deposition during the Cretaceous (Pohl et al., 2019) and derived $A_{platform}$ from the paleogeographical maps.

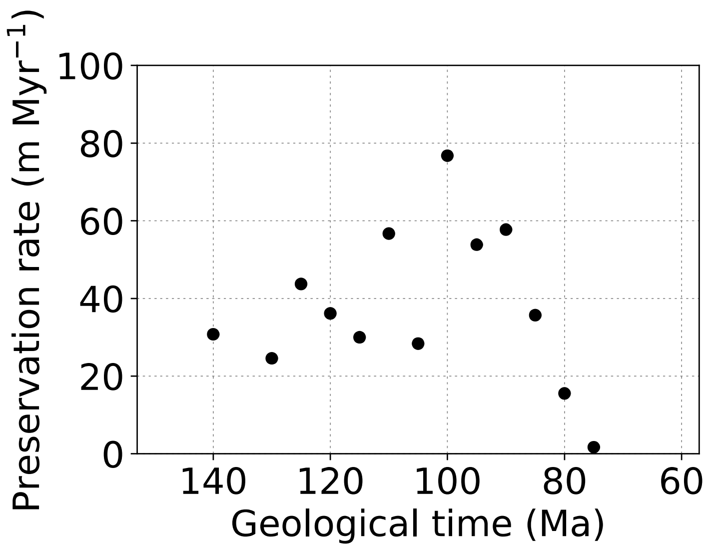

Figure S1. Mean preservation rates calculated using time bins of 5 m.y.

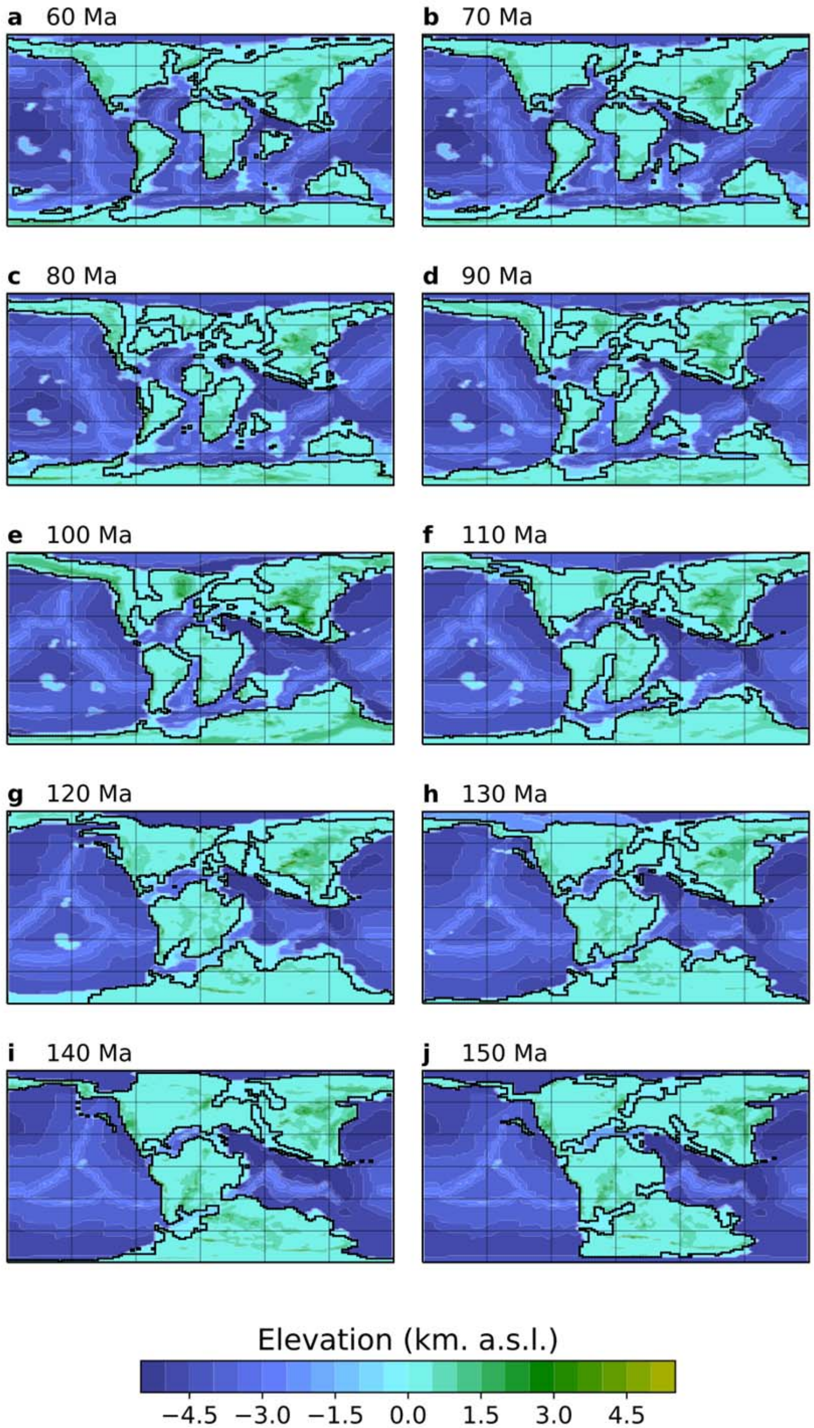

Figure S2. Continental reconstructions used in the GEOCLIM model (Scotese, 2016; Scotese and Wright, 2018).

REFERENCES CITED

Bosscher, H., and Schlager, W., 1993, Accumulation rates of carbonate platforms: The Journal of Geology, v. 101, p. 345–355, https://doi.org/10.1086/648228.

Donnadieu, Y., Goddéris, Y., Pierrehumbert, R., Dromart, G., Fluteau, F., and Jacob, R., 2006, A GEOCLIM simulation of climatic and biogeochemical consequences of Pangea breakup: Geochemistry Geophysics Geosystems, v. 7, p. Q11019 http://doi.wiley.com/10.1029/2006GC001278, https://doi.org/10.1029/2006GC001278.

Gradstein, F.M., Ogg, J.G., Schmitz, M., and Ogg, G., eds., 2012, The Geologic Time Scale, Volumes 1 & 2: Elsevier.

Jacob, R.L., 1997, Low frequency variability in a simulated atmosphere-ocean system: University of Wisconsin Madison, 170 p.

Pohl, A., Laugié, M., Borgomano, J., Michel, J., Lanteaume, C., Scotese, C.R., Frau, C., Poli, E., and Donnadieu, Y., 2019, Quantifying the paleogeographic driver of Cretaceous carbonate platform development using paleoecological niche modeling: Palaeogeography, Palaeoclimatology, Palaeoecology, v. 514, p. 222–232, https://doi.org/10.1016/j.palaeo.2018.10.017.

Ridgwell, A., 2005, A Mid Mesozoic Revolution in the regulation of ocean chemistry: Marine Geology, v. 217, p. 339–357, https://doi.org/10.1016/j.margeo.2004.10.036.

Ridgwell, A., and Zeebe, R., 2005, The role of the global carbonate cycle in the regulation and evolution of the Earth system: Earth and Planetary Science Letters, v. 234, p. 299–315, https://doi.org/10.1016/j.epsl.2005.03.006.

Scotese, C.R., 2016, PALEOMAP PaleoAtlas for GPlates and the PaleoData Plotter Program (PALEOMAP Project, 2016): https://www.earthbyte.org/paleomap-paleoatlas-for-gplates/.

Scotese, C.R., and Wright, N., 2018, PALEOMAP Paleodigital Elevation Models (PaleoDEMS) for the Phanerozoic (PALEOMAP Project, 2018): https://www.earthbyte.org/paleodem-resource- scotese-and-wright-2018/.

Suchéras-Marx, B., Mattioli, E., Allemand, P., Giraud, F., Pittet, B., Plancq, J., and Escarguel, G., 2019, The colonization of the oceans by calcifying pelagic algae: Biogeosciences, v. 16, p. 2501–2510, https://doi.org/10.5194/bg-16-2501-2019.

Walker, L.J., Wilkinson, B.H., and Ivany, L.C., 2002, Continental drift and Phanerozoic carbonate accumulation in shallow-shelf and deep-marine settings: The Journal of Geology, v. 110, p. 75–87, https://doi.org/10.1086/324318.

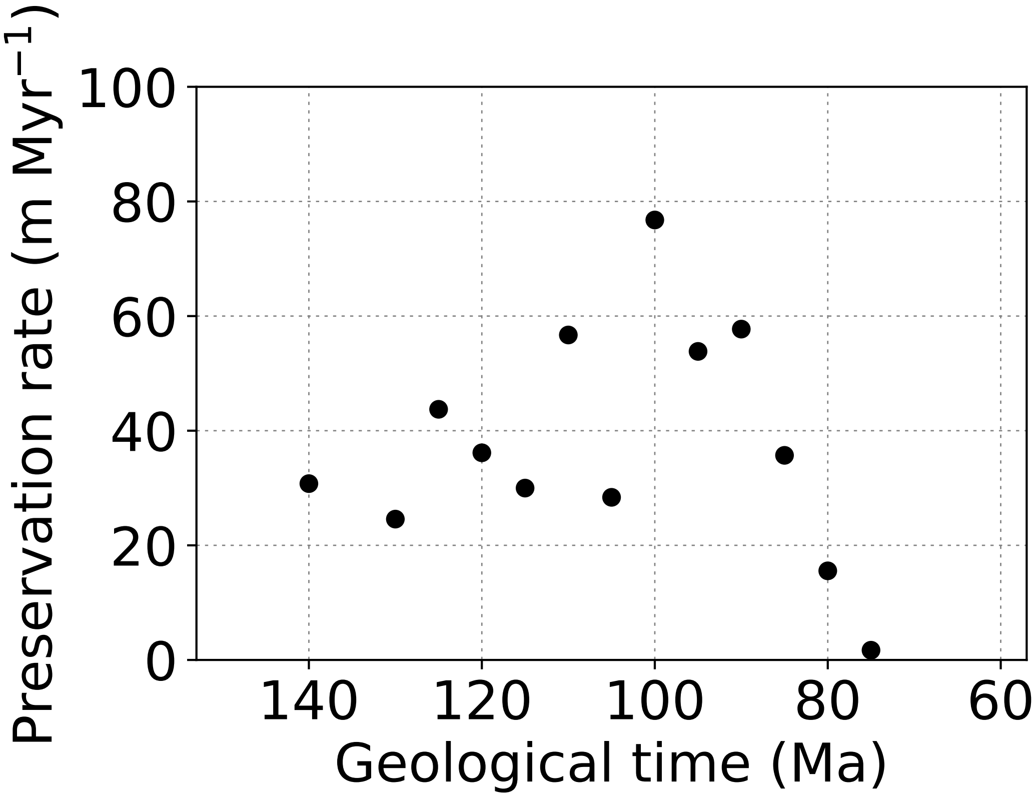
Preservation rate (m Myr^{-1})
100
80
60
40
20
0
140
120
100
80
60
Geological time (Ma)

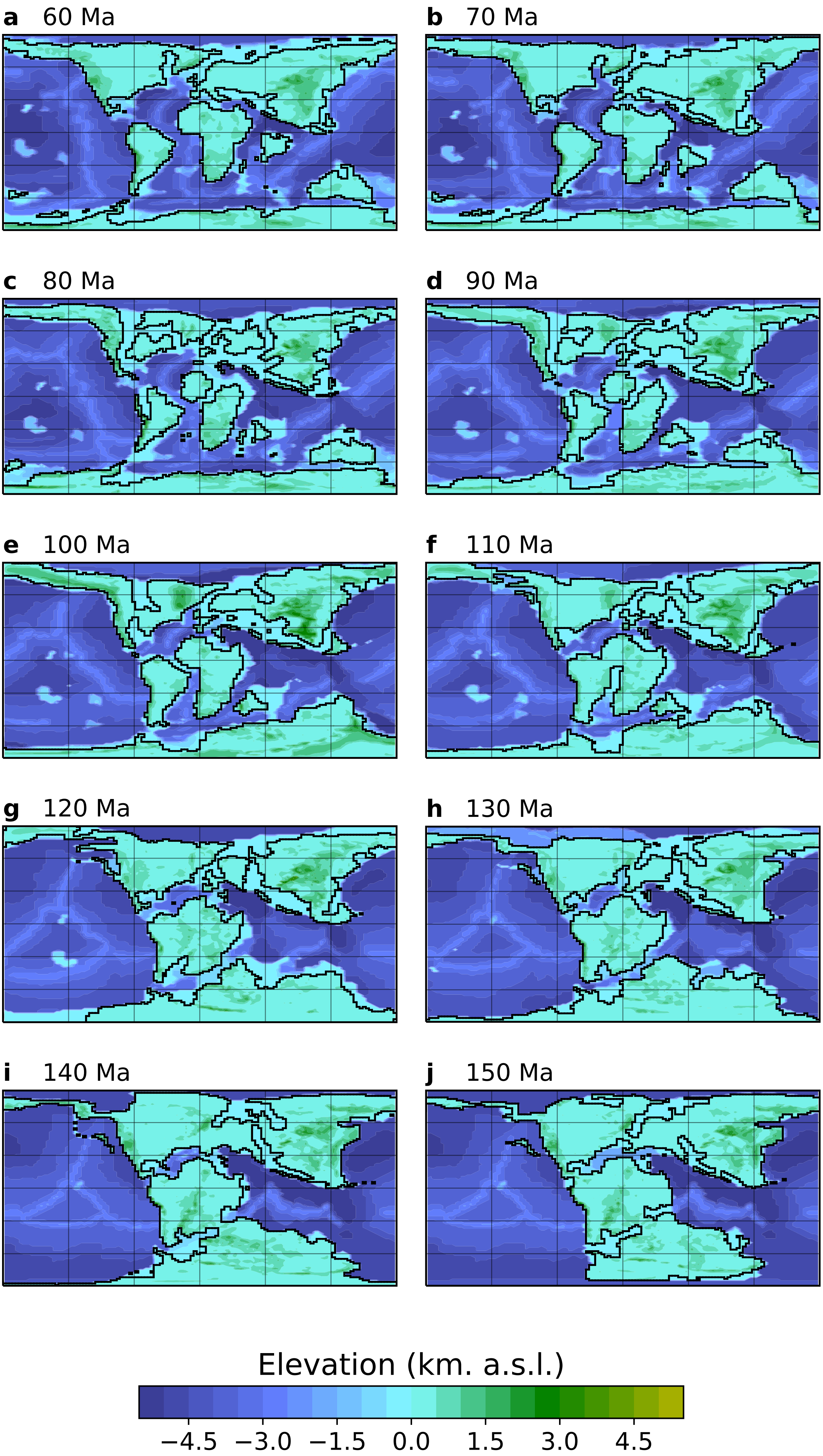
a 60 Ma
b 70 Ma
c 80 Ma
d 90 Ma
e 100 Ma
f 110 Ma
g 120 Ma
h 130 Ma
i 140 Ma
j 150 Ma
Elevation (km. a.s.l.)
−4.5
−3.0
−1.5
0.0
1.5
3.0
4.5

Experiment name	Globally-averaged, mean annual surface air temperature (°C)
60Ma_140ppm	2.042
60Ma_210ppm	4.612
60Ma_280ppm	15.43
60Ma_420ppm	17.18
60Ma_560ppm	18.36
60Ma_840ppm	20.27
60Ma_1120ppm	21.47
60Ma_2240ppm	24.61
60Ma_4480ppm	28.6
70Ma_280ppm	5.737
70Ma_420ppm	6.936
70Ma_560ppm	16.63
70Ma_840ppm	18.98
70Ma_1120ppm	20.38
70Ma_2240ppm	23.83
70Ma_4480ppm	27.5
80Ma_140ppm	7.369
80Ma_210ppm	9.103
80Ma_280ppm	15.41
80Ma_420ppm	16.7
80Ma_560ppm	18.43
80Ma_840ppm	21.65
80Ma_1120ppm	22.99
80Ma_2240ppm	26.08
80Ma_4480ppm	29.3
90Ma_70ppm	1.581
90Ma_140ppm	14.94
90Ma_210ppm	16.24
90Ma_280ppm	17.26
90Ma_420ppm	18.6
90Ma_560ppm	19.56
90Ma_840ppm	20.93
90Ma_1120ppm	22.36
90Ma_2240ppm	25.84
90Ma_4480ppm	29.52
100Ma_140ppm	0.8807
100Ma_210ppm	16.01
100Ma_280ppm	16.86
100Ma_420ppm	18.51
100Ma_560ppm	19.41
100Ma_840ppm	21.11
100Ma_1120ppm	22.23
100Ma_2240ppm	25.78
100Ma_4480ppm	29.42

Experiment name	Globally-averaged, mean annual surface air temperature (°C)
110Ma_140ppm	3.921
110Ma_210ppm	6.52
110Ma_280ppm	14.1
110Ma_420ppm	16.33
110Ma_560ppm	17.77
110Ma_840ppm	19.4
110Ma_1120ppm	20.77
110Ma_2240ppm	24.1
110Ma_4480ppm	27.92
120Ma_140ppm	2.022
120Ma_210ppm	6.712
120Ma_280ppm	14.26
120Ma_420ppm	16.12
120Ma_560ppm	17.33
120Ma_840ppm	19.09
120Ma_1120ppm	20.51
120Ma_2240ppm	24.18
120Ma_4480ppm	28.1
130Ma_560ppm	8.58
130Ma_650ppm	14.66
130Ma_740ppm	15.81
130Ma_840ppm	16.75
130Ma_1120ppm	17.78
130Ma_2240ppm	21.84
130Ma_4480ppm	26.38
130Ma_8960ppm	30.81
140Ma_560ppm	6.4
140Ma_840ppm	9.089
140Ma_930ppm	9.787
140Ma_1020ppm	15.98
140Ma_1120ppm	16.6
140Ma_2240ppm	20.38
140Ma_4480ppm	24.5
140Ma_8960ppm	29.45
150Ma_560ppm	6.842
150Ma_840ppm	8.407
150Ma_1120ppm	11.23
150Ma_1210ppm	15.06
150Ma_1305ppm	16.79
150Ma_1400ppm	17.32
150Ma_1680ppm	18.39
150Ma_1960ppm	19.75
150Ma_2240ppm	20.37
150Ma_4480ppm	24.35
150Ma_8960ppm	28.87